Bayesian estimation of the scaling parameter of fixational eye movements

ARTICLE *in* EPL (EUROPHYSICS LETTERS) · DECEMBER 2012

Impact Factor: 2.27 · DOI: 10.1209/0295-5075/100/40003

4 AUTHORS, INCLUDING:

N. Makarava

Physikalisch-Technische Bundesanstalt

7 PUBLICATIONS **14** CITATIONS

SEE PROFILE

Mario Bettenbühl

Universität Potsdam

5 PUBLICATIONS **41** CITATIONS

SEE PROFILE

Ralf Engbert

Universität Potsdam

124 PUBLICATIONS **3,152** CITATIONS

SEE PROFILE

Bayesian estimation of the scaling parameter of fixational eye movements

2012 EPL 100 40003

(http://iopscience.iop.org/0295-5075/100/4/40003)

A Letters Journal Exploring the Frontiers of Physics

November 2012

EPL, **100** (2012) 40003
doi: 10.1209/0295-5075/100/40003

www.epljournal.org

Bayesian estimation of the scaling parameter of fixational eye movements

Natallia Makarava[1], Mario Bettenbühl[1,2], Ralf Engbert[2] and Matthias Holschneider[1]

[1] *Interdisciplinary Center for Dynamics of Complex Systems, University of Potsdam - Karl-Liebknecht-Str. 24, 14476 Potsdam, Germany, EU*
[2] *Cognitive Science Program, University of Potsdam - Karl-Liebknecht-Str. 24, 14476 Potsdam, Germany, EU*

received 11 June 2012; accepted in final form 9 November 2012
published online 3 December 2012

PACS 05.10.-a – Computational methods in statistical physics and nonlinear dynamics
PACS 87.19.lt – Sensory systems: visual, auditory, tactile, taste, and olfaction
PACS 89.75.Da – Systems obeying scaling laws

Abstract – In this study we re-evaluate the estimation of the self-similarity exponent of fixational eye movements using Bayesian theory. Our analysis is based on a subsampling decomposition, which permits an analysis of the signal up to some scale factor. We demonstrate that our approach can be applied to simulated data from mathematical models of fixational eye movements to distinguish the models' properties reliably.

Introduction. – Since the 17th century, researchers showed a particular interest to study different aspects of eye movements. Jurin [1] was the first who discovered that the eyes continue to perform miniature eye movements while human observers fixate a static target. Nowadays, video-based recordings of eye movements renewed the scientific interest in these fixational eye movements [2–4]. It is well established that different components of fixational eye movements (FEM) are classified as tremor, drift, and microsaccades [5–8] (cf. fig. 1). The two most important components of fixational eye movements are i) physiological drift, a slow random component that could be characterized as a diffusion process, and ii) microsaccades, rapid small-amplitude movements for which it is unclear if they are generated by the same mechanism as physiological drift or by a separate generating process. Tremor is a small-amplitude, oscillatory component superimposed to drift that cannot be resolved with video-based recording devices used in the current study.

The detection [2,9,10], the characterization [9,11–13] or modeling of the underlying generating dynamics [14–17] of FEM has been a topic of many studies. Recently, Engbert and Kliegl [18] suggested that fixational eye movements might be interpreted as realizations of a fractional Brownian motion (fBm) (see also [19]). The so-called Hurst exponent, which parametrizes fBm, indicates its correlation behavior and allows the detection of the long-range dependences inside the signal.

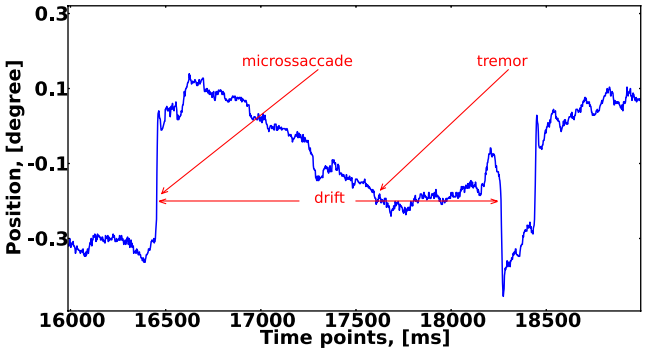

Fig. 1: (Colour on-line) Example of fixational eye movements. The most important components drift and microsaccades are quite visible. Tremor is a very small-amplitude oscillatory component.

There are several standard techniques used for the estimation of the Hurst exponent in the literature, *e.g.*, the R/S analysis proposed by Hurst himself [20], detrended fluctuation analysis (DFA) [21], standard deviation analysis (SDA) [22], Whittle estimator [23], and a wavelet-based approach [24]. Recently, some of the authors proposed a Bayesian approach for the estimation of the Hurst exponent from Gaussian data [25]. A similar analysis was also proposed by Conti *et al.* for the study of telecom networks [26]. The advantages of the Bayesian approach

over the existing estimation techniques are as follows: i) it is possible to calculate the point estimator and confidence intervals simultaneously; ii) the analysis could be applied successfully to short data sets as well as to unevenly sampled data; iii) the method outperforms standard measures as DFA, periodogram and wavelet-based estimator (for comparison, see [25,27,28]). FEM have been investigated so far using DFA and SDA approaches as in [29,30], and a change of the scaling behavior from a persistent behavior on short time scales to an anti-persistent behavior on long time scales was observed.

In this work, we investigate the estimation problem for the Hurst exponent from a sequence of increments of a discrete process over some scale. This allows us to examine the value of the Hurst exponent on different levels according to the scale factor. With this approach, the Hurst exponent keeps its value constant for a sampled sequence of fBm at all scale levels. In order to test this property on FEM data we examine both, experimental and simulated FEM data. In the first case, the existence of the scale level starting from which the data acquire the anti-persistent behavior, turning the signal into short-memory process, is shown. Additionally, we demonstrate that the Bayesian approach permits a reliable estimation of the Hurst exponent based on different trials from the same participant.

Moreover, we also validate the proposed method on simulated time series, mimicking the FEM based on a time-delayed random-walk model [29] and a model based on a self-avoiding walk [31] that generates both slow movements and microsaccades.

Basic definitions. – Fractional Brownian motion, $\{B^H(t), t\in\mathbb{R}\}$, plays a central role in theory of self-similar stochastic processes. It is well established for modeling the natural phenomena which exhibit self-similar behavior in various areas such as finance [32,33], economics [34], hydrology [20,35], turbulence or traffic [36–38], and behavioral neuroscience [39,40].

Fractional Brownian motion (fBm) is a non-stationary Gaussian process that exhibit self-similarity behavior according to the following expression [41,42]:

$$B^H(\alpha t) =_d \alpha^H B^H(t), \tag{1}$$

where the sign $=_d$ denotes the equivalence of the finite-dimensional distributions. The above equation holds for any $\alpha>0$. Standard normalized fBm starts at zero $B^H(0)=0$ and has a zero mean $\mathbb{E}(B^H(t))=0$. This process is therefore fully characterized by its covariance function at time points t and u [43,44],

$$\mathbb{E}(B^H(t)B^H(u)) = \frac{1}{2}(|t|^{2H}+|u|^{2H}-|t-u|^{2H}). \tag{2}$$

The parameter H, known as the Hurst exponent, is a free parameter of the process [20]. It takes values from the interval $]0,1[$ and characterizes the (Hölder) regularity

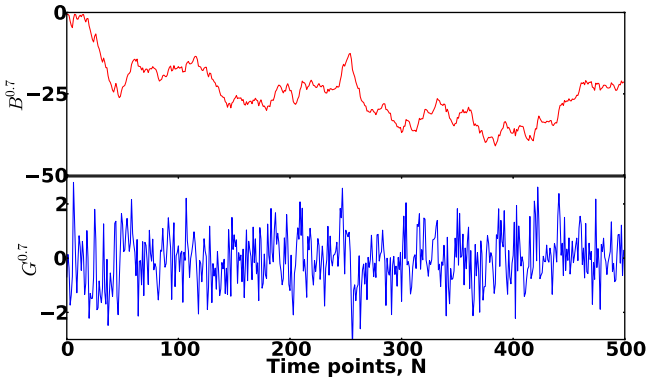

Fig. 2: (Colour on-line) Top: simulation of fractional Brownian motion of length $N=500$ and $H=0.7$. Bottom: fractional Gaussian noise driven as an increment process of fractional Brownian motion of length $N=500$ and $H=0.7$. The difference in correlation structure is clearly visible.

of the process [43]. The case of $H=1/2$ represents the Brownian motion.

Fractional Brownian motion has stationary increments, *i.e.*, its increments [45],

$$G_s^H(t) = B^H(t+s) - B^H(t), \qquad t\in\mathbb{R},$$

form a stationary process for any fixed $s>0$. That means that the joint probability distribution does not change when shifted in time or space, *i.e.*,

$$B^H(t+s) - B^H(t) =_d B^H(t) - B^H(0). \tag{3}$$

Now, self-similarity implies that

$$G_{\alpha s}^H(\alpha t) = B^H(\alpha t+\alpha s) - B^H(\alpha t) = \alpha^H G_s^H(t). \tag{4}$$

Next, considering the discrete process

$$g_{s,n}^H = G_s^H(ns) = B^H([n+1]s) - B^H(ns), \tag{5}$$

it follows that $g_{\alpha s,n}^H = \alpha^H g_{s,n}^H$, and thus, all the increment processes are the same up to a multiplicative factor. We therefore take

$$g_n^H = B^H(n+1) - B^H(n) \tag{6}$$

as the reference discrete Gaussian increment process. We call this process the discrete fractional Gaussian noise process (fGn). Figure 2 shows the comparison of fBm and fGn with a fixed Hurst exponent of $H=0.7$.

Discrete fractional Gaussian noise is a stationary process in discrete time with auto-covariance function,

$$\begin{aligned}\rho(k) &= \mathbb{E}(g_{n+k}^H \cdot g_n^H)\\ &= \frac{1}{2}(|k-1|^{2H} - 2|k|^{2H} + |k+1|^{2H}).\end{aligned} \tag{7}$$

In the case of $H=1/2$, fGn represents a sequence of independent and identically distributed Gaussian random

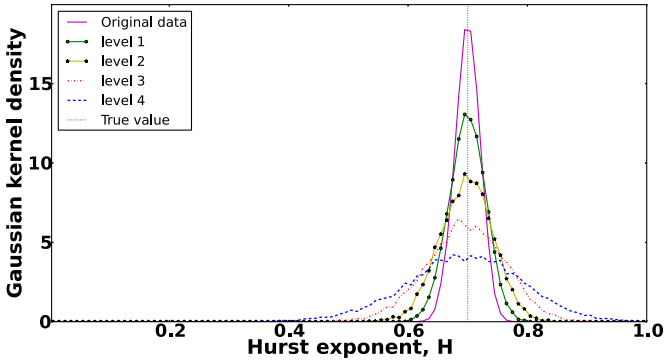

Fig. 3: (Colour on-line) Gaussian kernel density of the maximal point estimator of the Hurst exponent received by the Bayesian approach for fGn. The original value of the Hurst exponent is fixed to $H = 0.7$.

variables. For all other cases, the auto-covariance function behaves asymptotically as power function for large k. However, for $1/2 < H < 1$, the auto-covariance function tends to zero slowly, so that $\sum_{k=-\infty}^{\infty} \rho(k)$ diverges. In this case the process exhibits long-range dependences. For $0 < H < 1/2$, $\sum_{k=-\infty}^{\infty} \rho(k) = 0$ and the process exposes the so-called "negative dependence".

Model and methods. – In order to analyze the scale dependence of the Hurst exponent of a sampled signal we propose the following approach: given a discrete signal d_n, for any discrete scale $a \in \{1, 2, \ldots\}$ we consider the sequence of increments over the scale a:

$$D_{a,n} = d_{[n+1]a} - d_{na}.$$

This can be regarded as a discrete wavelet transform with respect to the rather singular wavelet $\delta_1 - \delta_0$, which justifies the identification of a as a scale. We now propose to analyze the dependence of the Hurst exponent on the level j corresponding to the scale $a = 2^j$ by applying a fGn-based Bayesian analysis to each of these signals, as outlined below. Note that for a sampled sequence of Brownian motion, the current analysis would yield a constant Hurst exponent across all levels (fig. 3). Our analysis therefore provides a mean of discriminate homogeneous, scale invariant processes for which the correlation structure depends on the scale.

The studies of the scaling behaviors of FEM by DFA and SDA [18,29] detected two different types on short and long time scales: persistent behavior on the short time scale and anti-persistence on the long one. In this work, we approach the estimation task via the implementation of the Bayes theorem [46],

$$\mathbb{P}(A|B) = \frac{\mathbb{P}(B|A)\,\mathbb{P}(A)}{\mathbb{P}(B)},$$

to the model

$$X_n = \lambda g_n^H + \beta, \quad n = 1, 2, \ldots, \tag{8}$$

Table 1: The 95% confidence interval for $\hat{H}$ for artificial fGn with $H = 0.7$.

Level	95% confidence interval
Original data	$[0.658, 0.741]$
level 1	$[0.639, 0.759]$
level 2	$[0.611, 0.784]$
level 3	$[0.568, 0.824]$
level 4	$[0.502, 0.88]$
level 5	$[0.386, 0.99]$
True value	0.7

where g_n^H is the fGn and $H \in]0, 1[$ is the Hurst exponent, $\lambda > 0$, $\lambda \in \mathbb{R}$ is the amplitude, and $\beta \in \mathbb{R}$ is the offset.

Applying the Bayes theorem with Jeffreys-like prior [47] for the scale parameter λ and flat priors for all other parameters, we obtain the posterior distribution of the Hurst exponent H, *i.e.*,

$$\mathbb{P}(H|X) = \frac{C}{\gamma |\Sigma_H|^{1/2}\, R^{N-1}}. \tag{9}$$

Here, C is a normalization constant. The residuum R^2 and the mode β^* depend on H via $R^2 = X^t \Sigma_H^{-1} X - \gamma^2 \beta^{*2}$, $\beta^* = \frac{F^t \Sigma_H^{-1} X}{\gamma^2}$, $\gamma^2 = F^t \Sigma_H^{-1} F$, $F^t = [1, \ldots, 1]$. The advantage of this approach is that additionally to the point estimator, we also receive the confidence interval of the estimator.

In fig. 3 the results for the estimation of the Hurst exponent are shown. Here, we simulate data of fGn of length $N = 1000$, and perform 10000 realizations using the Monte Carlo simulation method. For each realization we estimate the Hurst exponent value of the subsampled time series according to the eq. (9), using a sliding window of length $N = 150$ when the length of the data is above 300, and N equals the data length elsewhere. Next, the data are decomposed up to scale level $j = 5$. Since increasing the level by one reduces the length of the time series to one-half, the time series at scale level $j = 5$ corresponds to a length of $N = 32$ data samples. Additionally, the 95% confidence intervals for the estimated Hurst exponent values according to the scale levels are given in table 1.

Fixational eye movements data. – The method proposed here is next applied to experimental FEM data (detailed information on experimental setup can be found in [9,10,29,48]) for which it has been shown that it can be described significantly well using fBm [18,19]. The data used for our investigations was collected in one session for each of the 24 participants (average age of 22 years). In each session, participants were asked to fixate a dot of black 3×3 pixels on white background on a computer display. Eye movements have been video-based recorded with an EyeLink II system at a sampling frequency of 500 Hz. Each participant was required to perform 30 trials of 20 seconds each. We used 622 trials after visual inspection for data loss based on eye blinking.

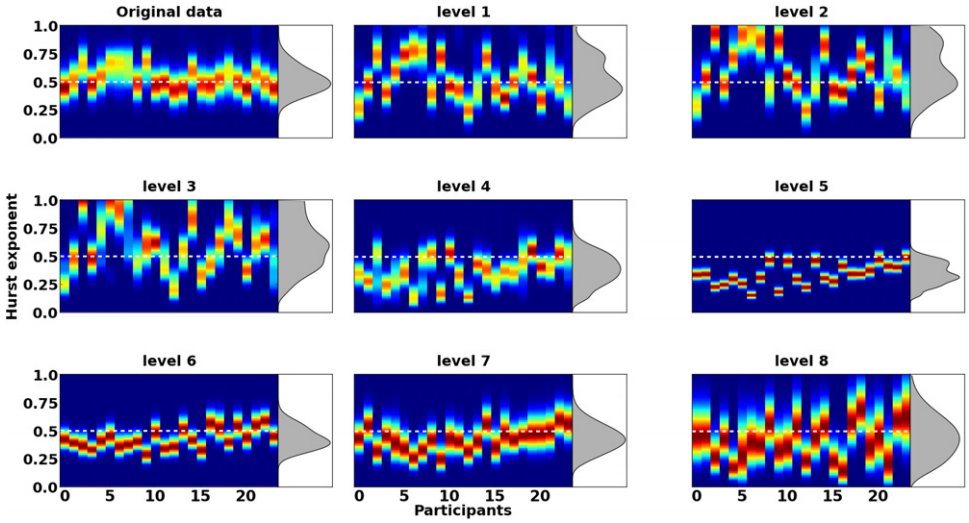

Fig. 4: (Colour on-line) Bayesian estimation of the Hurst exponent for time series of fixational eye movements. The analysis applied on different scales corresponding to the subsampling decomposition. White dotted lines denote the value of the Hurst exponent which equals 0.5.

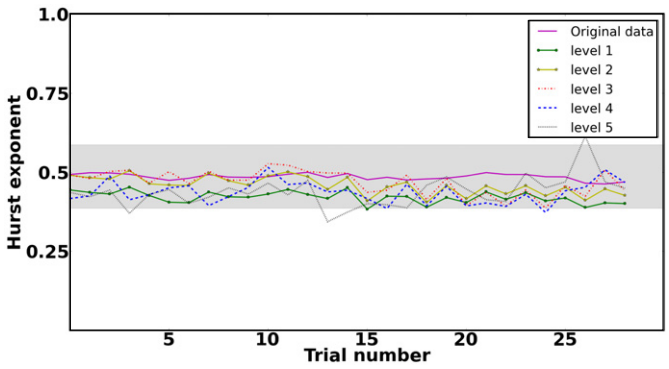

Fig. 5: (Colour on-line) Hurst exponent estimation for one of the participants of *Group I*. The gray area denotes the 10% error bar.

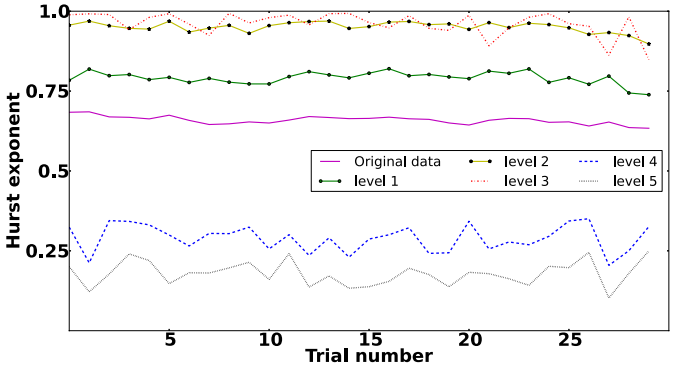

Fig. 6: (Colour on-line) Hurst exponent estimation for one of the participants of *Group III*. The independence of the Hurst exponent from the trial is clearly visible.

Next, we removed the microsaccades by an amplitude scale-invariant detection method [9], leaving us with trial durations between 15.98 and 19.88 seconds and investigate only the drift movements.

Although the Bayesian estimation can be used without data-preprocessing, in this case, a certain preprocessing step is necessary in order to use the increment series of FEM, since the underlying process in our model is fGn. Next, we perform the estimation of the Hurst exponent as described in the previous section, using a sliding window of $N = 150$ samples length (up to scale level 6). We obtain time series on 8 scale levels in addition to the original time series.

We estimate the value of the Hurst exponent as $H \approx 0.5$ for the original, complete time series (fig. 4). For the scale levels $j = 1$ to 3, we observe persistent behavior for more than half of the participants, since the Hurst exponent is $H > 0.5$. However, starting from scale level 4, the estimated values of the Hurst exponent make a significant transition into anti-persistence area ($H < 0.5$). This is especially visible for the data at level $j = 5$. For larger scales, the estimator oscillates near the value of $H = 0.5$. However, the location of the maximum of the posterior values of the Hurst exponent is still in the anti-persistent region for the majority of the tested participants.

As shown previously, the Hurst exponent for fBm does not change its value for different scale levels. However, for FEM data, the observed results can be divided into 3 different groups: *Group I*: the estimation of the Hurst exponent keep its value constant for 3 participants within a 10% error over the mean value (this is shown in fig. 5); *Group II*: the results are qualitatively comparable to the one in fig. 5, except that instead of 10%, a 20% error interval is necessary to describe changes of the Hurst exponent (this holds for 11 participants, data are not shown here). In contrast to this, the remaining 10 participants (*Group III*) show significantly different behavior, because values of the Hurst exponent for different scale levels are different (see fig. 6). However, for participants from each of the 3 different groups, the estimation of the Hurst exponent indicates

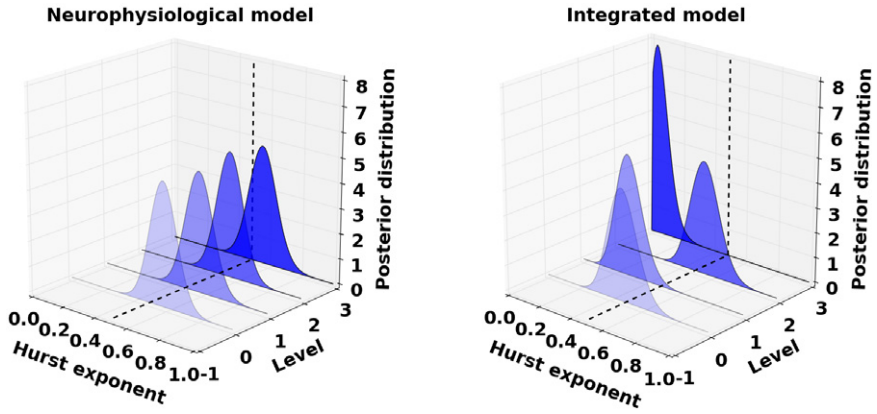

Fig. 7: (Colour on-line) Estimation of the Hurst exponent for two simulating models of fixational eye movements. Left: model of fixational eye movements data with neurophysiological delays; right: an integrated model of fixational eye movements.

persistence over different trials. We therefore speculate that the FEM data do not fully resemble the properties of fBm.

Simulated eye movements data. – Next, we apply the proposed method to analyze simulated time series, generated from the random-walk model of FEM with neurophysiological delays [29] and from an integrated model of slow FEM and microsaccades [31], which is based on a self-avoiding random walk.

Neurophysiological delay model. A delayed random-walk model [31] is based on neurophysiological delays. The model is intended to mimic the experimentally observed persistent behavior on short time scales [29]. The equation of motion of the model consists of three terms: an autoregressive term, a noise term, and a term with negative feedback, *i.e.*,

$$w_{i+1} = (1-\gamma)w_i + \xi_i - \lambda(\epsilon w_{i-\tau}), \tag{10}$$

where the autoregressive term $(1-\gamma)w_i$ generates the persistent correlations at the short time scales; the noise term ξ_i is Gaussian noise with $\langle \xi_i \rangle = 0$ and $\langle \xi_i \xi_j \rangle = \sigma^2 \delta_{ij}$; and $\lambda(\epsilon w_{i-\tau})$ generates the anti-persistent behavior on the long time scale. λ is the feedback strength, ϵ is the parameter for variation of the stepness of the control function, and τ is the physiological delay. The positions of the eye are represented in the following form:

$$x_{i+1} = x_i + w_{i+1} + \eta_i, \tag{11}$$

where η_i is an additive noise term with $\langle \eta_i \rangle = 0$ and $\langle \eta_i \eta_j \rangle = \rho^2 \delta_{ij}$ and standard deviation ρ. We use parameters as proposed in [29] ($\gamma = 0.25$, $\lambda = 0.15$, $\sigma = 0.075$, $\rho = 0.35$, $\epsilon = 1.1$, and $\tau = 70$) to produce 1000 realizations of length $N = 200000$ (one iteration step corresponds to 1 ms). Only the last 10000 values were taken into consideration to remove possible transient effects.

Integrated model of FEM. Here, the model of FEM is described by a self-avoiding random walk in a potential: the walker always moves to the minimum of the sum of the activation. We use here as well the parameters as proposed in [31]: the data are simulated on a lattice of 51 cells, the center is at $(25, 25)$ with slope parameter equal to 1. We produce 1000 realizations of length $N = 10000$ each.

To apply the Bayesian method for the Hurst exponent estimation in both cases, we calculate the Hurst exponent from subsampled time series of the increment processes as described previously. The estimation was implemented by a sliding window of length $N = 150$ along the time series. In fig. 7, the estimated values for the Hurst exponent at the different scale levels are shown. Here, the Hurst exponent values of the original simulated data are the same as for the real data of FEM ($H \approx 0.5$). Moreover, for the neurophysiological model, the Hurst exponent keeps this value for all scale levels and does not show any changes in memory. However, this is not fully observed with the integrated model. Here, the transition to the anti-persistent area at level 2 is detected. Such kind of behavior was also observed with the real data of FEM. Thus, our analysis suggests that the integrated model is compatible with the experimental data, showing qualitatively the same behavior. Results for both models are plotted in fig. 7.

Conclusions. – In this paper we analyzed the scaling exponent of FEM data using a Bayesian approach. We applied the Bayesian method to subsampled data of fixational eye movements. This approach allowed us to conclude that FEM data do not fully resemble the properties of fBm. Given the results, we conclude that starting from a specific scale level, the Hurst exponent changes its value and the signal turns from the persistent to the anti-persistent area. Additionally, it was shown that the values of the Hurst exponent are unique for all participants. The validation of the method on simulated models of FEM showed that the integrated model demonstrates scaling behavior which is in good agreement with the scaling behavior observed in real data of FEM.

REFERENCES

[1] Jurin J., *A Compleat System of Opticks in Four Books*, edited by Smith R. (1738).
[2] Engbert R. and Kliegl R., *Vision Res.*, **43** (2003) 1035.
[3] Martinez-Conde S., Macknik S. L. and Hubel D. H., *Nat. Neurosci.*, **3** (2000) 251.
[4] Martinez-Conde S., Macknik S. L. and Hubel D. H., *Nat. Rev. Neurosci.*, **5** (2004) 229.
[5] Cornsweet T. N., *J. Opt. Soc. Am.*, **46** (1956) 987.
[6] Ditchburn R. W., *Vision Res.*, **20** (1980) 271.
[7] Rolfs M., *Vision Res.*, **49** (2009) 2415.
[8] Martinez-Conde S., Macknik S. L., Troncoso X. G. and Hubel D. H., *Trends Neurosci.*, **32** (2009) 463.
[9] Bettenbühl M., Paladini C., Mergenthaler K., Kliegl R., Engbert R. and Holschneider M., *J. Eye Mov. Res.*, **3** (2010) 1.
[10] Engbert R. and Mergenthaler K., *Proc. Natl. Acad. Sci. U.S.A.*, **103** (2006) 7192.
[11] Abadi R. V., Scallan C. J. and Clement R. A., *Vision Res.*, **40** (2000) 2813.
[12] Abadi R. V. and Gowen E., *Vision Res.*, **44** (2004) 2675.
[13] Moshel S., Liang J.-R., Caspi A., Engbert R., Kliegl R., Havlin S. and Zivotofsky A. Z., *Ann. N. Y. Acad. Sci.*, **1039** (2005) 484.
[14] Bettenbühl M., Rusconi M., Engbert R. and Holschneider M., *Markov models for sequences of microsaccades*, Conference Abstract BC11, *Computational Neuroscience and Neurotechnology Bernstein Conference and Neurex Annual Meeting 2011* (Frontiers in Computational Neuroscience) 2011.
[15] Hafed Z. M., *Eur. J. Neurosci.*, **33** (2011) 2101.
[16] Otero-Millan J., Serra A., Leigh R. J., Troncoso X. G., Macknik S. L. and Martinez-Conde S., *J. Neurosci.*, **31** (2011) 4379.
[17] Otero-Millan J., Macknik S., Serra A., Leigh R. and Martinez-Conde S., *Ann. N. Y. Acad. Sci.*, **1233** (2011) 107.
[18] Engbert R. and Kliegl R., *Psychol. Sci.*, **15** (2004) 431.
[19] Liang J.-R., Moshel S., Zivotofsky A. Z., Caspi A., Engbert R., Kliegl R. and Havlin S., *Phys. Rev. E*, **71** (2005) 031909.
[20] Hurst H. E., *Trans. Am. Soc. Civil Eng.*, **116** (1951) 770.
[21] Peng C.-K., Buldyrev S., Havlin S., Simons M., Stanley H. E. and Goldberger A., *Phys Rev E*, **49** (1994) 1685.
[22] Allegrini P., Barbi M., Grigolini P. and West B. J., *Phys. Rev. E*, **52** (1995) 5281.
[23] Whittle P., *J. R. Stat. Soc., Ser. B (Methodol.)*, **15** (1953) 125.
[24] Abry P. and Veitch D., *IEEE Trans. Inf.*, **44** (1998) 2.
[25] Makarava N., Benmehdi S. and Holschneider M., *Phys. Rev. E*, **84** (2011) 021109.
[26] Conti P. L., Lijoi A. and Ruggeri F., *Appl. Stoch. Models Bus. Ind.*, **20** (2004) 305.
[27] Benmehdi S., Makarava N., Benhamidouche N. and Holschneider M., *Nonlinear Processes Geophys.*, **18** (2011) 441.
[28] Makarava N. and Holschneider M., *Eur. Phys. J. B*, **85** (2012) 272.
[29] Mergenthaler K. and Engbert R., *Phys. Rev. Lett.*, **98** (2007) 138104.
[30] Moshel S., Zivotofsky A. Z., Liang J.-R., Engbert R., Kurths J., Kliegl R. and Havlin S., *Eur. Phys. J. ST*, **161** (2008) 207.
[31] Engbert R., Mergenthaler K., Sinn P. and Pikovsky A., *Proc. Natl. Acad. Sci. U.S.A.*, **108** (2011) E765.
[32] Bartolozzi M., Mellen C., Matteo T. D. and Aste T., *Eur. Phys. J. B*, **58** (2007) 207.
[33] Matos J.-A., Gama S., Ruskin H., Sharkasi A. and Crane M., *Physica A*, **387** (2008) 3910.
[34] Benth F. E., *Appl. Math. Finance*, **10** (2003) 303.
[35] Molz F. J., Liu H. H. and Szulga J., *Water Resour. Res.*, **33** (1997) 2273.
[36] Véhel J. L. and Riedi R., *Fractional brownian motion and data traffic modeling: The other end of the spectrum*, in *Proceedings of Fractals in Engineering* (Springer) 1997, pp 185–202 .
[37] Willinger M., Taqqu M. S., Leland W. E. and Wilson D. V., *Stat. Sci.*, **10** (1995) 67.
[38] Conti P. L., De Giovanni L. and Naldi M., *Comput. Netw.*, **54** (2010) 2626.
[39] Collins J. J. and Luca C. J. D., *Exp. Brain Res.*, **103** (1995) 151.
[40] Churilla A. M., Gottschalke W. A., Liebovitch L. S., Selector L. Y., Todorov A. T. and Yeandle S., *Ann. Biomed. Eng.*, **24** (1996) 99.
[41] Kolmogorov A. N., *Dokl. Akad. Nauk SSSR*, **26** (1940) 115.
[42] Mandelbrot B. B. and Ness J. W. V., *SIAM Rev.*, **10** (1968) 422.
[43] Biagini F., Hu Y., Oksendal B. and Zhang T., *Stochastic Calculus for Fractional Brownian Motion and Applications* (Springer, London) 2008.
[44] Decreusefond L. and Üstünel A., *ESAIM: Proc.*, **5** (1998) 75.
[45] Samorodnitsky G. and Taqqu M. S., *Stable Non-Gaussian Random Processes* (Chapman and Hall, New York) 1994.
[46] Bayes T. and Price R., *Philos. Trans. R. Soc. London*, **53** (1763) 370.
[47] Jeffreys H., *Proc. R. Soc. London, Ser. A*, **186** (1946) 453.
[48] Bettenbühl M., Rusconi M., Engbert R. and Holschneider M., *PLoS ONE*, **7** (2012) e43388.